Mon. Not. R. Astron. Soc. **381,** 1702–1710 (2007) doi:10.1111/j.1365-2966.2007.12342.x

The neutrino emission due to plasmon decay and neutrino luminosity of white dwarfs

E. M. Kantor★ and M. E. Gusakov★
Ioffe Physical Technical Institute, Politekhnicheskaya 26, St Petersburg 194021, Russia

Accepted 2007 August 14. Received 2007 August 10; in original form 2007 July 4

ABSTRACT
One of the effective mechanisms of neutrino energy losses in red giants, pre-supernovae and in the cores of white dwarfs is the emission of neutrino–antineutrino pairs in the process of plasmon decay. In this paper, we numerically calculate the emissivity due to plasmon decay in a wide range of temperatures 10^7–10^{11} K and densities $(2 \times 10^2$–$10^{14})\,\mathrm{g\,cm^{-3}}$. Numerical results are approximated by convenient analytical expressions. We also calculate and approximate by analytical expressions the neutrino luminosity of white dwarfs due to plasmon decay, as a function of their mass and internal temperature. This neutrino luminosity depends on the chemical composition of white dwarfs only through the parameter μ_e (the net number of baryons per electron) and is the dominant neutrino luminosity in all white dwarfs at the neutrino cooling stage.

Key words: neutrinos – white dwarfs.

1 INTRODUCTION

It is well known that neutrino emission plays an important role in the evolution of red giants, pre-supernovae, white dwarfs and neutron stars. Neutrinos appear in a number of reactions in dense stellar matter (see e.g. Yakovlev et al. 2001) and freely escape from the star, producing a powerful mechanism of their cooling. One of the effective neutrino generation mechanisms is the plasmon decay.

In contrast to ordinary photons in vacuum, plasmons, which are quanta of electromagnetic field in a plasma, can be not only transverse (in this case two polarization vectors of plasmon are perpendicular to wavevector), but longitudinal as well. The longitudinal plasmons appear in the theory as a result of quantization of the well-known Langmuir plasma waves.

Plasmon can decay into a neutrino–antineutrino pair, $\gamma \to \nu + \overline{\nu}$. The appropriate neutrino emissivity was analysed in a series of papers since 1963, when Adams, Ruderman & Woo (1963) had suggested this mechanism of energy losses in dense stellar matter for the first time. An account of these papers and references can be found in the review by Yakovlev et al. (2001) as well as in a recent paper by Odrzywołek (2007). Here we discuss in more detail only three papers which summarize and extend the results of previous works.

Itoh et al. (1992) calculated the emissivity due to plasmon decay as a function of temperature and density and presented a table of numerical values and an approximate fitting formula. Unfortunately, this approximate formula does not reproduce analytical asymptotes for the emissivity and thus can be applied only in a restricted region of temperatures and densities (near the maximum value of the emissivity). In addition, when calculating the emissivity, Itoh et al. (1992) used approximate expressions for the dielectric functions of electron gas and for plasmon dispersion relations which can be justified only at low enough temperatures (in a strongly degenerate electron gas).

On the contrary, Braaten & Segel (1993) started with the most general expressions for the neutrino emissivity due to plasmon decay. They did not make any assumptions concerning degeneracy of the electron gas while calculating the dielectric functions and plasmon dispersion relations. To simplify their analysis, Braaten & Segel (1993) suggested an elegant scheme to calculate approximately the dielectric functions, dispersion relations and the neutrino emissivity. However, these authors did not present any tables with their numerical results or any approximate formula for the emissivity. Therefore, it is difficult to use their results in applications.

Using the approximate method of Braaten & Segel (1993), Haft et al. (1994) calculated the emissivity due to plasmon decay and fitted it by an analytical formula. This formula accurately describes the emissivity in a range of temperatures and densities where the plasmon decay is the most important neutrino emission mechanism. However, the fitting expression of Haft, Raffelt & Weiss (1994) does not satisfy the analytical asymptotes for the emissivity (they are presented in Section 2).

In this paper we would like to fill in the gaps in the literature devoted to the subject. We will (i) numerically calculate the neutrino emissivity due to plasmon decay making no assumptions concerning degeneracy or relativity of the electron gas; (ii) employ the approximate scheme of Braaten & Segel (1993) and find a fitting expression

★E-mail: kantor@mail.ioffe.ru (EMK); gusakov@astro.ioffe.ru (MEG)

for the emissivity which reproduces the correct asymptotes. Thus, our main goal is to facilitate the use of the data on the neutrino emission due to plasmon decay.

The paper is organized as follows. In Section 2 we present general equations describing the neutrino energy-loss rate owing to plasmon decay. In Section 3 we give the fitting expression for the plasma frequency which is a key parameter because the asymptotes of the emissivity depend on it. In Section 4 we present the fitting expressions for the emissivity. In Section 5 we apply the results of the preceding sections and find an analytical formula describing the neutrino luminosity of white dwarfs as a function of their mass and internal temperature. We summarize in Section 6. In Appendix A we present expressions for the dielectric functions of the electron–positron plasma. Finally, in Appendix B we describe a table of our numerical results.

2 GENERAL EQUATIONS

The neutrino emissivity due to plasmon decay can be presented as a sum of three components: the longitudinal component Q_l (due to decay of longitudinal plasmons); the transverse component Q_t (the decay of transverse plasmons governed by the vector part of the weak interaction Hamiltonian) and the axial component Q_A (the decay of transverse plasmons governed by the axial part of the weak interaction Hamiltonian). The component Q_A is small and can be neglected (see e.g. Kohyama et al. 1994).

The emissivities Q_t and Q_l (per unit volume) are given in the form of integrals (see e.g. Braaten 1991; Braaten & Segel 1993):

$$Q_\mathrm{t} = 2\, Q_0\, \frac{\hbar^9}{m_\mathrm{e}^9 c^{15}} \int_0^\infty \mathrm{d}k\, k^2 Z_\mathrm{t}(k) \left(\omega_\mathrm{t}^2 - k^2c^2\right)^3 n_\mathrm{B}(\omega_\mathrm{t}), \tag{1}$$

$$Q_\mathrm{l} = Q_0\, \frac{\hbar^9}{m_\mathrm{e}^9 c^{15}} \int_0^{k_\mathrm{max}} \mathrm{d}k\, k^2 Z_\mathrm{l}(k) \left(\omega_\mathrm{l}^2 - k^2c^2\right)^3 n_\mathrm{B}(\omega_\mathrm{l}). \tag{2}$$

Here, the integration is carried over the plasmon wavenumber k. In equations (1) and (2) $Q_0 = [(m_\mathrm{e}c)^9/\hbar^{10}][G_\mathrm{F}^2/(96\pi^4\alpha)](\sum_\nu C_\mathrm{V}^2) \approx 1.3858\times10^{21}$ erg s^{-1} cm^{-3}; $G_\mathrm{F} = 1.436 \times 10^{-49}$ erg cm^3 is the Fermi weak coupling constant; $\alpha = e^2/(\hbar c) \approx 1/137$ is the fine structure constant; e and m_e are the electron charge and mass, respectively; $\hbar$ is the Planck constant; c is the speed of light; $\sum_\nu C_\mathrm{V}^2 \approx 0.9248$ is the sum of squared normalized vector constants C_V over all neutrino flavours. Furthermore, $\omega_\mathrm{t}(k)$ and $\omega_\mathrm{l}(k)$ are, respectively, the frequencies of transverse and longitudinal plasmons, which depend on the wavenumber k; $Z_\mathrm{t}(k)^{-1} \equiv \partial(\omega_\mathrm{t}^2\epsilon_\mathrm{t})/\partial(\omega_\mathrm{t}^2)$; $Z_\mathrm{l}(k)^{-1} \equiv (\omega_\mathrm{l}^2 - k^2c^2)\, \partial\epsilon_\mathrm{l}/\partial(\omega_\mathrm{l}^2)$, where ϵ_t and ϵ_l are the transverse and longitudinal dielectric functions of the electron–positron plasma, respectively. Finally, $n_\mathrm{B}(\omega_\mathrm{t,l}) = 1/\{\exp[\hbar\omega_\mathrm{t,l}/(k_\mathrm{B}T)] - 1\}$ is the Bose–Einstein distribution function for transverse or longitudinal plasmons; T is the temperature; k_B is the Boltzmann constant; k_max is the maximum wavenumber at which the decay of longitudinal plasmon is still kinematically allowed by energy and momentum conservation laws.

In the astrophysical literature the emissivity is presented as a function of temperature T and the effective mass density $\tilde{\rho}$, given by

$$\tilde{\rho} \equiv \rho/\mu_\mathrm{e}, \tag{3}$$

where ρ is the actual mass density; $\mu_\mathrm{e} = \sum_i A_i n_i/(\sum_i Z_i n_i)$ is the net number of baryons per electron; Z_i and A_i are, respectively, the charge and mass numbers of atomic nucleus species i; n_i is the number density of these species. Note that at densities higher than the neutron drip density $\rho_\mathrm{d} \approx 4 \times 10^{11}$ g cm^{-3}, free neutrons must be taken into account in the sum over i, in addition to atomic nuclei, when calculating μ_e.

It is straightforward to verify that $\tilde{\rho}$ can be rewritten as

$$\tilde{\rho} \approx (n_\mathrm{e} - n_{\mathrm{e}^+})\, m_\mathrm{u}. \tag{4}$$

Here, n_e and n_{e^+} are the number densities of electrons and positrons; m_u is the a.m.u.

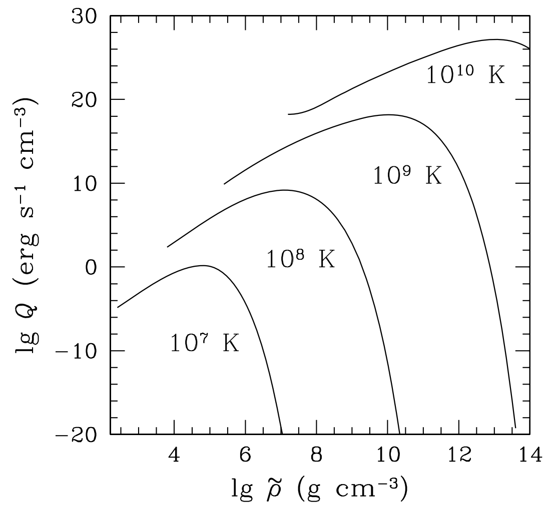

Figure 1. The emissivity $Q = Q_\mathrm{t} + Q_\mathrm{l}$ versus $\tilde{\rho}$ for $T = 10^7, 10^8, 10^9$ and 10^{10} K.

The dependence of the emissivity $Q = Q_\mathrm{t} + Q_\mathrm{l}$ on $\tilde{\rho}$ for temperatures $T = 10^7, 10^8, 10^9$ and 10^{10} K is presented in Fig. 1. As seen from the figure, at fixed $\tilde{\rho}$ the emissivity increases with the growth of T. If we fix T, the dependence $Q(\tilde{\rho})$ has a maximum. In the vicinity of the maximum the plasma frequency of the electron–positron plasma ω_p is of the order of temperature, $\hbar\omega_\mathrm{p} \sim k_\mathrm{B}T$ (see Section 5 for details). At high temperatures and low densities the emissivity ceases to depend on $\tilde{\rho}$ (see equations 6, 10 and 11 below). In the figure this situation is illustrated by the upper curve, which is plotted for $T = 10^{10}$ K. One sees that at $\tilde{\rho} < 10^8$ g cm^{-3} the curve tends to be horizontal.

As follows from equations (1) and (2), for calculation of Q_t and Q_l one needs to know the dispersion relations for transverse and longitudinal plasmons, $\omega_\mathrm{l}(k)$ and $\omega_\mathrm{t}(k)$, as well as the dielectric functions $\epsilon_\mathrm{t}(\omega, k)$ and $\epsilon_\mathrm{l}(\omega, k)$. We calculated the dielectric functions $\epsilon_\mathrm{t}(\omega, k)$ and $\epsilon_\mathrm{l}(\omega, k)$ for a wide range of densities and temperatures in the random phase approximation and numerically obtained the dispersion relations and the plasma frequency ω_p. The equations we used to compute the dielectric functions of the electron–positron plasma are given in Appendix A. These results were applied to calculate the integrals (1) and (2). In these calculations, we did not make any simplifying assumptions concerning the degree of degeneracy or relativity of the electron gas. The table with our numerical results can be found on the web, http://www.ioffe.ru/astro/NSG/plasmon/table.dat (file table.dat). This table is described in Appendix B.

The emissivities Q_l and Q_t depend on two parameters characterizing stellar matter. For example, one may choose T and n_e or T and $\tilde{\rho}$ as proper parameters. Following previous results (see e.g. Itoh et al. 1992), we take T and $\tilde{\rho}$ as independent variables. It is convenient to introduce the notation $f \equiv \hbar\omega_\mathrm{p}/(k_\mathrm{B}T)$.

The expression for the plasma frequency in the Braaten–Segel approximation has the form (see Braaten & Segel 1993)

$$\omega_\mathrm{p}^2 = \frac{4\alpha}{\pi}\,\frac{c^3}{\hbar^2}\int_0^\infty \mathrm{d}p\;\frac{p^2}{E}\left(1-\frac{1}{3}v^2\right)[n_\mathrm{F}(E)+\overline{n}_\mathrm{F}(E)]\,, \tag{5}$$

where p, $v = pc/E$ and $E = \sqrt{p^2c^2 + m_\mathrm{e}^2c^4}$ are, respectively, the momentum, dimensionless velocity and energy of an electron or positron; $n_\mathrm{F}(E) = 1/\{\exp[(E-\mu)/(k_\mathrm{B}T)]+1\}$ is the Fermi–Dirac distribution for electrons; $\overline{n}_\mathrm{F}(E) = 1/\{\exp[(E+\mu)/(k_\mathrm{B}T)]+1\}$ is the Fermi–Dirac distribution for positrons; μ is the electron chemical potential.

In the region of relativistic temperatures ($k_\mathrm{B}T \gg m_\mathrm{e}c^2$) and under the condition $k_\mathrm{B}T \gg p_\mathrm{F}c$, the plasma frequency (5) has the asymptote

$$\omega_\mathrm{p}^2 = \frac{4\pi\alpha}{9}\,\frac{(k_\mathrm{B}T)^2}{\hbar^2}. \tag{6}$$

Here $p_\mathrm{F} \equiv (3\pi^2\hbar^3 n_\mathrm{e})^{1/3}$. For a degenerate electron gas p_F is the usual Fermi momentum of the electrons.

In the case when (i) the electron gas is degenerate ($k_\mathrm{B}T \ll \sqrt{p_\mathrm{F}^2c^2 + m_\mathrm{e}^2c^4} - m_\mathrm{e}c^2$ and the contribution of positrons to ω_p can be neglected), or (ii) the gas is non-degenerate, non-relativistic, and the temperature is not too high for the appearance of positrons (see e.g. Landau & Lifshitz 1980, section 105), expression (5) reduces to

$$\omega_\mathrm{p}^2 = \frac{4\alpha}{3\pi}\,\frac{c^3}{\hbar^2}\,\frac{p_\mathrm{F}^3}{\sqrt{p_\mathrm{F}^2c^2+m_\mathrm{e}^2c^4}}. \tag{7}$$

If the gas is non-relativistic ($p_\mathrm{F} \ll m_\mathrm{e}\,c$), then this equation gives the well-known result, $\omega_\mathrm{p}^2 = 4\pi e^2 n_\mathrm{e}/m_\mathrm{e}$. Note that since the contribution of the positrons to the asymptote (7) is negligible ($n_{\mathrm{e}^+} \ll n_\mathrm{e}$), p_F in this case can be approximately calculated as $p_\mathrm{F} \approx [3\pi^2\hbar^3\,(n_\mathrm{e} - n_{\mathrm{e}^+})]^{1/3} = (3\pi^2\hbar^3\,\tilde{\rho}/m_\mathrm{u})^{1/3}$ (see equation 4). Introducing a new dimensionless parameter, $\tilde{p}_\mathrm{F} \equiv (\hbar/m_\mathrm{e}c)\,(3\pi^2\,\tilde{\rho}/m_\mathrm{u})^{1/3}$, one can substitute $(m_\mathrm{e}c\,\tilde{p}_\mathrm{F})$ for p_F in the asymptote (7).

Braaten & Segel (1993) developed a useful approximate method to calculate the emissivity due to plasmon decay. Below in this section we present some results obtained using this method (more details are given in the original paper of the authors).

Using the method of Braaten & Segel (1993), the emissivity can be expressed through the parameter v_*, which is a characteristic dimensionless velocity of electrons scaling from 0 in the non-relativistic limit to 1 in the ultrarelativistic limit,

$$v_* = \frac{\omega_1}{\omega_\mathrm{p}}. \tag{8}$$

Here, the plasma frequency ω_p is given by equation (5) while the frequency ω_1 is

$$\omega_1^2 = \frac{4\alpha}{\pi}\,\frac{c^3}{\hbar^2}\int_0^\infty \mathrm{d}p\;\frac{p^2}{E}\left(\frac{5}{3}v^2 - v^4\right)[n_\mathrm{F}(E)+\overline{n}_\mathrm{F}(E)]\,. \tag{9}$$

In two limiting cases the neutrino emissivity due to decay of longitudinal and transverse plasmons can be calculated analytically. If the plasma frequency is much smaller than the temperature [$f \equiv \hbar\omega_\mathrm{p}/(k_\mathrm{B}T) \ll 1$], then equations (1) and (2) can be simplified and written as

$$Q_\mathrm{t} = Q_0\left(\frac{k_\mathrm{B}T}{m_\mathrm{e}c^2}\right)^9\;4\zeta_3\,\beta^6\,f^6, \tag{10}$$

$$Q_\mathrm{l} = Q_0\left(\frac{k_\mathrm{B}T}{m_\mathrm{e}c^2}\right)^9\;A(v_*)\,f^8. \tag{11}$$

Here, $\zeta_3 \simeq 1.202\,057$ is a value of the Riemann ζ-function and the function $\beta(v_*)$ equals

$$\beta = \left[\frac{3}{2v_*^2}\left(1 - \frac{1-v_*^2}{2v_*}\,\ln\frac{1+v_*}{1-v_*}\right)\right]^{1/2}. \tag{12}$$

In the non-relativistic limit ($v_* \to 0$) it reduces to $\beta = 1$, while in the ultrarelativistic limit ($v_* \to 1$) one has $\beta = \sqrt{3/2}$. Furthermore, $A(v_*)$ is a smooth function of v_*, changing from 8/105 ≈ 0.076 at $v_* \to 0$ to 0.349 at $v_* \to 1$. If the plasma frequency is much greater than the temperature ($f \gg 1$), then the integrals (1) and (2) can be taken analytically,

$$Q_\mathrm{t} = Q_0\left(\frac{k_\mathrm{B}T}{m_\mathrm{e}c^2}\right)^9\;b_1\,f^{7.5}\exp(-f), \tag{13}$$

$$Q_\mathrm{l} = Q_0\left(\frac{k_\mathrm{B}T}{m_\mathrm{e}c^2}\right)^9\;b_2\,f^{7.5}\exp(-f), \tag{14}$$

where $b_1 = \sqrt{2\pi}\,(1+v_*^2/5)^{-3/2}$ and $b_2 = \sqrt{\pi/2}\,(3v_*^2/5)^{-3/2}$.

3 FIT FOR PLASMA FREQUENCY

To simplify subsequent analysis we derived an analytical formula which approximates the plasma frequency (5) in a wide range of temperatures $T = 10^7$–10^{11} K and effective densities $\tilde{\rho} = (2\times10^2$–$10^{14})$ g cm^{-3}. This range of parameters includes all possible limiting cases of degenerate, ultrarelativistic, as well as of non-degenerate non-relativistic electron gas. We calculated the emissivity on a dense grid of mesh points (with the steps 0.2 in $\log T$ and $\log\tilde{\rho}$). The rms relative error of our approximation is 0.4 per cent. The maximum error of 1.4 per cent is at $\log T = 9.0$ (K) and $\log\tilde{\rho} = 2.4$ (g cm^{-3}). The fit reproduces the asymptotes from Section 2. The squared plasma frequency can be approximated as

$$\omega_\mathrm{p}^2 = \left(\frac{m_\mathrm{e}\,c^2}{\hbar}\right)^2\sqrt{\mathrm{asy}_2^2 + [\mathrm{asy}_1\,(1-C\;D)]^2}. \tag{15}$$

Here, $\mathrm{asy}_1 = 4\alpha/(3\pi)\;\tilde{p}_\mathrm{F}^3/\sqrt{1+\tilde{p}_\mathrm{F}^2}$ is exactly the low-temperature asymptote (7) [we recall that $\tilde{p}_\mathrm{F} = (\hbar/m_\mathrm{e}c)\;(3\pi^2\tilde{\rho}/m_\mathrm{u})^{1/3}$], while asy_2 is given by

$$\mathrm{asy}_2 = \frac{4\pi\alpha}{9}\,p_2\left(\frac{t^2}{p_2}+1+\frac{p_2}{t^2}\right)\left[1+\frac{p_3}{(t/\sqrt{p_2})^{p_1}}\right]^{-10}, \tag{16}$$

with $t \equiv k_\mathrm{B}\,T/(m_\mathrm{e}c^2)$. In the high-temperature limit, asy_2 transforms into the asymptote (6). The fitting parameters p_1, p_2 and p_3 equal 1.793, 0.0645 and 0.433, respectively.

The function C in equation (15) is written as

$$C = 1 - c_2\,\frac{(c_1\,t)^2}{1+(c_1\,t)^2}, \tag{17}$$

where

$$c_1 = p_4\,\frac{1+p_5\,\tilde{\rho}^{p_6}}{1+p_7\,(1+p_5\,\tilde{\rho}^{p_6})}, \tag{18}$$

$$c_2 = p_8 + p_9\frac{\tilde{\rho}}{p_{10}+\tilde{\rho}}, \tag{19}$$

with $p_4 = 0.011\,39, p_5 = 2.484\times10^6$, $p_6 = -0.6195, p_7 = 0.000\,9632$, $p_8 = 0.4372, p_9 = 1.614$ and $p_{10} = 8.504\times10^8$.

At low temperatures the plasma frequency in the first approximation depends only on $\tilde{\rho}$ and we have $C = 1$. The function D in equation (15) has the form

$$D = \frac{t^2}{d_1\sqrt{1+(d_2\,t)^2}}, \tag{20}$$

$$d_1 = \frac{6}{\pi^2}\,\frac{\tilde{p}_{\rm F}^2(1+\tilde{p}_{\rm F}^2)}{2\tilde{p}_{\rm F}^2+5}, \qquad d_2 = \frac{\pi^2}{6}\,\frac{1}{\sqrt{1+\tilde{p}_{\rm F}^2}-1}. \tag{21}$$

At high temperatures (when $t \gg 1$ and the electron gas is non-degenerate) the fit (15) reproduces the high-temperature asymptote (6). At low temperatures (a degenerate gas or a non-degenerate non-relativistic gas; positrons can be neglected) the fit (15) transforms into the analytical asymptote (7), which depends only on $\tilde{\rho}$. The function D is designed in such a way to reproduce not only the asymptote (7) of plasma frequency but also the first temperature corrections to $\omega_{\rm p}$. For a degenerate electron gas, the expansion parameter is $k_{\rm B}T/\mu$; for the non-degenerate non-relativistic gas it reduces to $k_{\rm B}T/(m_{\rm e}c^2)$.

4 FIT FOR THE NEUTRINO EMISSIVITY

In this section we present an analytical formula which approximates the results of numerical calculations of the emissivity $Q = Q_{\rm t} + Q_{\rm l}$ (per unit volume) and reproduces the asymptotes from Section 2. The approximation was made in a range of temperatures $T = 10^7$–10^{11} K and effective densities $\tilde{\rho} = (2\times10^2$–$10^{14})$ g cm^{-3}. The emissivity $Q(\tilde{\rho}, T)$ was calculated on the same grid points as the plasma frequency (Section 3). At $f \equiv \hbar\,\omega_{\rm p}/(k_{\rm B}T) > 20$ the accuracy of our fit is only logarithmic. However, in this case the emissivity Q is exponentially small, $Q \sim \exp(-f)$.

The fit for the emissivity can be presented in the form

$$Q = Q_{\rm l} + Q_{\rm t} = Q_0 t^9\,(W_{\rm t} + W_{\rm l})\exp(-f), \tag{22}$$

where, as before, $t \equiv k_{\rm B}T/(m_{\rm e}\,c^2)$ and we define

$$W_{\rm t} \equiv {\rm asy}_{\rm t1} + {\rm asy}_{\rm t2}\exp\left[\frac{q_3}{(f^{q_1}+q_2)}\right], \tag{23}$$

$$W_{\rm l} \equiv \frac{{\rm asy}_{\rm l2}\left[{\rm asy}_{\rm l1} + q_4\left(1+q_5\,v_*^{2.5}\right)^{3.5} f^9\right]}{{\rm asy}_{\rm l2} + \left[{\rm asy}_{\rm l1} + q_4\left(1+q_5\,v_*^{2.5}\right)^{3.5} f^9\right]}. \tag{24}$$

In equations (23) and (24)

$${\rm asy}_{\rm t1} = a_1 f^6, \qquad {\rm asy}_{\rm l1} = a_2 f^8, \tag{25}$$

$${\rm asy}_{\rm t2} = b_1 f^{7.5}, \qquad {\rm asy}_{\rm l2} = b_2 f^{7.5}, \tag{26}$$

$$a_1 = 4\zeta_3\beta^6, \qquad a_2 = \frac{8}{105} + \left(0.349 - \frac{8}{105}\right)v_*^{10}; \tag{27}$$

the functions $b_1(v_*)$ and $b_2(v_*)$ are the same as in equations (13) and (14); the function $\beta(v_*)$ is given by equation (12). At $f \ll 1$ equation (22) transforms into

$$Q = Q_{\rm t} = Q_0 t^9 {\rm asy}_{\rm t1} = Q_0 t^9\,4\zeta_3\beta^6 f^6 \tag{28}$$

(compare with the asymptotes 10 and 11). At $f \gg 1$ one has

$$Q = Q_0 t^9({\rm asy}_{t2} + {\rm asy}_{l2})\exp(-f) = Q_0 t^9 (b_1 + b_2) f^{7.5}\exp(-f) \tag{29}$$

(compare with the asymptotes 13 and 14).

When calculating the emissivity from equation (22) one should use fit (15) for the plasma frequency $\omega_{\rm p}$ and the following fit for the characteristic velocity v_*,

$$v_* = \left(\frac{\tilde{v}_{\rm F}^3 + s_1\,t^{s_2}\tilde{\rho}^{s_3}}{1 + s_1\,t^{s_2}\tilde{\rho}^{s_3}}\right)^{1/3}, \tag{30}$$

where $\tilde{v}_{\rm F} \equiv \tilde{p}_{\rm F}/\sqrt{1+\tilde{p}_{\rm F}^2}$; $s_1 = 9.079$; $s_2 = 1.399$; $s_3 = -0.065\,92$. The rms relative error of this approximate formula in the chosen range of T and $\tilde{\rho}$ constitutes 1.4 per cent. The maximum fitting error is equal to 5.4 per cent at $\log T = 8.4$ (K) and $\log\tilde{\rho} = 3.8$ (g cm^{-3}).

In addition, it turns out to be necessary to use a special approximate formula for the function $\beta^6(v_*)$ from which the fitting expression (22) depends on [a simple substitution of equation (30) into (12) and subsequent calculation of β^6 results in large errors]

$$\beta^6 = \beta^6(\tilde{v}_{\rm F}) + \left[3.375 - \beta^6(\tilde{v}_{\rm F})\right]\frac{t^{r_2}\tilde{\rho}^{r_3}}{(r_1 + t^{r_2}\tilde{\rho}^{r_3})}, \tag{31}$$

where $r_1 = 0.3520$; $r_2 = 1.195$; $r_3 = -0.1060$. The rms relative error of this fit constitutes 2.5 per cent, the maximum error of 8.3 per cent is at $\log T = 9.6$ (K) and $\log\tilde{\rho} = 5.0$ (g cm^{-3}). The function (31) was approximated in the same temperature and density range as the parameter v_* and the emissivity Q.

The use of approximate formulae (15) and (30)–(31) leads to the following values of fitting parameters $q_1, \ldots, q_5$ (see equations 23 and 24), minimizing rms deviation of the emissivity, provided by equation (22), from the numerical values,

$$q_1 = 0.7886,\ q_2 = 0.2642,$$
$$q_3 = 1.024,\ q_4 = 0.078\,39,\ q_5 = 0.1784. \tag{32}$$

The rms relative error of the approximate formula (22) with these coefficients is 4 per cent, the maximum error is 7.9 per cent at $\log T = 8.4$ and $\log\tilde{\rho} = 6.4$.

In Fig. 2 we compare our numerical results for the emissivity $Q_{\rm num}$ with the results taken from the literature (corresponding emissivities are denoted as $Q_{\rm lit}$). The figure presents the relative deviation $\delta \equiv (Q_{\rm lit} - Q_{\rm num})/Q_{\rm num}$ as a function of $\tilde{\rho}$ for a set of temperatures $T = 10^7, 10^8, 10^9$ and 10^{10} K. The solid curves demonstrate relative deviations of the approximation (22), suggested in this paper, from our numerical results $Q_{\rm num}$; the long dashes show deviations from numerical calculations of Itoh et al. (1992) (taken from their table); the dotted curves correspond to relative deviations calculated using an approximate formula, suggested by Itoh et al. (1992); the short dashes describe relative deviations calculated from a fitting formula of Haft et al. (1994). Finally, by the dot–dashed curves we show relative deviations calculated from the approximate formula for the emissivity given in the review of Yakovlev et al. (2001). In that review it is recommended to use the formula only for $\tilde{\rho} > 10^8$ g cm^{-3} and for strongly degenerate electrons. From the analysis of Fig. 2 a number of conclusions can be inferred as follows.

(i) The approximate formula obtained in this section is in good agreement with the results of numerical calculations as long as $f < 20$ (at greater f, i.e. at higher densities, the solid curve tends to go upward).

(ii) Our calculations agree with results of Itoh et al. (1992) in the range of parameters, where the electron gas is strongly degenerate and the emissivity is not small. However, as follows, e.g. from Fig. 2 at $T = 10^9$ K, some our results deviate from those of Itoh et al. (1992) for $\tilde{\rho} \sim 10^{13}$ g cm^{-3}. For this case, matter is strongly degenerate so that the simplified assumptions, made by Itoh et al. for calculating the emissivity, could not lead to such deviations. [Let us note that Itoh et al. used the dielectric function, calculated by Jancovici (1962)

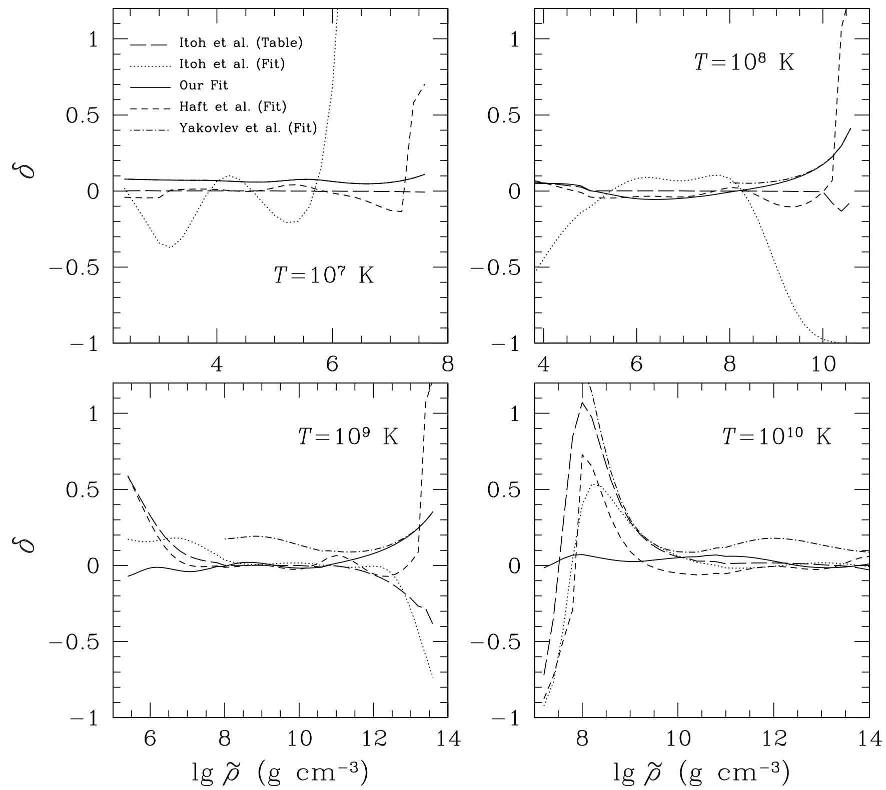

Figure 2. Relative deviation $\delta \equiv (Q_{\rm lit} - Q_{\rm num})/Q_{\rm num}$ versus $\tilde{\rho}$ for $T = 10^7, 10^8, 10^9$ and 10^{10} K. Here, $Q_{\rm num}$ is the emissivity, numerically calculated in this paper. For $Q_{\rm lit}$ we take one of the emissivities obtained either from the fitting formula (22) (solid lines); or from the table of Itoh et al. (1992) (long dashes); or from the fitting formula of Itoh et al. (1992) (dots); or from the fitting formula of Haft et al. (1994) (short dashes); or from the approximate formula from the review of Yakovlev et al. (2001) (dot–dashed lines).

for a strongly degenerate electron gas, see Appendix A.] Taking into account that our numerical results at such densities and $T = 10^9$ K do not differ from the analytical asymptote for the emissivity by more than 10 per cent, the results of Itoh et al. (1992) in the indicated parameter range seem less accurate than ours.

(iii) The fitting formula of Itoh et al. (1992) satisfactorily describes the results of numerical calculations only near the maximum of the emissivity (when $f \sim 1$).

(iv) The fitting formula of Haft et al. (1994) agrees well with our numerical results in the same region of temperatures and densities in which the numerical results of Itoh et al. (1992) agrees with our numerical results.

(v) The approximate formula from the review of Yakovlev et al. (2001) becomes inaccurate at high temperatures (i.e. $T = 10^{10}$ K) and low densities ($\tilde{\rho} \sim 10^8$ g cm^{-3}). This approximate formula is valid only for strongly degenerate electrons, while the electron degeneracy becomes mild at high T and low $\tilde{\rho}$.

Summarizing, as follows from Fig. 2, the results of various authors are in *satisfactory* agreement in the ranges of T and $\tilde{\rho}$ where the process of neutrino emission due to plasmon decay is the most efficient mechanism of energy losses in dense stellar matter.

5 THE NEUTRINO LUMINOSITY OF WHITE DWARFS

Let us apply the results of Section 4 to analyse the neutrino luminosity of white dwarfs. As will be argued below, the neutrino luminosity due to plasmon decay only weakly depends on a specific model of a white dwarf. Thus, it can be considered as a universal function of the white dwarf mass M and its internal temperature T. Here we calculate this universal function and approximate it by a convenient analytical formula.

As is well known, the thermal evolution of a white dwarf consists of two stages, the neutrino cooling stage (where cooling is mainly realized through the neutrino emission from the entire stellar body) and the photon stage (the main energy losses through the photon radiation from the stellar surface). A transition from one stage to the other occurs at the stellar age $\tau \sim (10^7$–$10^8)$ yr, when the surface temperature of a star equals $T_{\rm s} \sim 2.5 \times 10^4$ K (for a hydrogen or helium atmosphere white dwarf, see e.g. Winget et al. 2004).

At the neutrino cooling stage the main mechanism of energy losses is the neutrino emission due to plasmon decay (the second important process – the neutrino bremsstrahlung in collisions of electrons with atomic nuclei – is 10–100 times weaker, see Winget et al. 2004). We numerically calculated the neutrino luminosity $L_\nu(M, T)$ of white dwarfs caused by the decay of plasmons. When doing the calculation, we made the following assumptions. First, to obtain the density profile inside a white dwarf we assumed that the pressure is fully determined by degenerate electrons. Secondly, the stellar core was assumed to be isothermal, which is a good approximation for not too young white dwarfs ($\tau \gtrsim 10$–1000 yr). Thirdly, we neglected beta-captures when calculating the structure and luminosity of massive white dwarfs. Beta-captures lead to softening of the equation of state, and influence the hydrostatic structure of a star. In addition, they change stellar chemical composition, affect the number of nucleons per electron, $\mu_{\rm e}$, and, consequently, the quantities $\tilde{\rho}$ and L_ν. However, because the neutrino luminosity is the integral

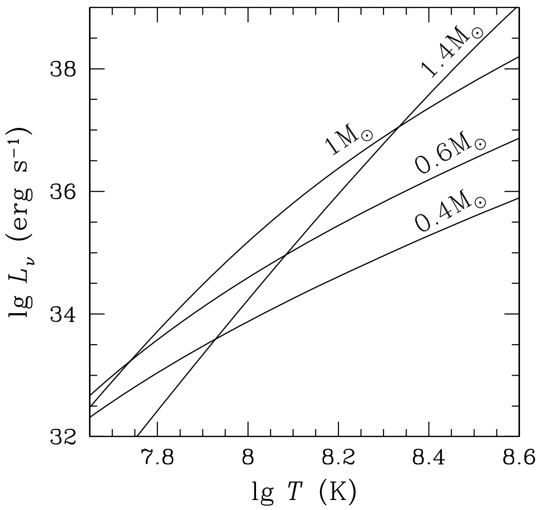

Figure 3. The neutrino luminosity L_ν versus internal stellar temperature T for white dwarfs with $M = 0.4, 0.6, 1.0$ and $1.4\,\mathrm{M}_\odot$.

characteristic of a star, it should not strongly depend on these simplified assumptions.

In Fig. 3 we present the neutrino luminosity L_ν as a function of stellar core temperature T for white dwarfs with the masses $M = 0.4, 0.6, 1.0$ and $1.4\,\mathrm{M}_\odot$.

The results of numerical calculations of L_ν in the range of temperatures $T = 3\times10^7$–5×10^8 K and masses $M = (0.4$–$1.3)\,\mathrm{M}_\odot$ were approximated by the formula

$$L_{\nu1}(M,T) = 10^{39}\,\frac{k_1 T_8^{31/3}(k_4\widetilde{M}^{k_2}+\widetilde{M}^{k_3})(1+k_5\widetilde{M})^{22/3}}{\left[k_6(1+k_5\widetilde{M})^{22/(3k_7)}T_8^{22/(3k_7)}+\widetilde{M}^{22/(3k_7)}\right]^{k_7}}\quad \mathrm{erg\,s^{-1}}, \tag{33}$$

where $\widetilde{M} = M/\mathrm{M}_\odot$, $T_8 = T/(10^8\ \mathrm{K})$, and

$$k_1 = 1.050,\ k_2 = 11.86,\ k_3 = 5.901,$$
$$k_4 = 1.010,\ k_5 = -0.5448,\ k_6 = 2.777,\ k_7 = 5.635. \tag{34}$$

For white dwarfs with $M = (1.3$–$1.4)\,\mathrm{M}_\odot$ the neutrino luminosity in the same range of temperatures $T = 3\times10^7$–5×10^8 K is given by

$$L_{\nu2}(M,T) = 10^{39}\,\frac{l_1 T_8^{31/3}\widetilde{M}^{l_2}}{\left[l_3 T_8^{22/(3l_5)}+\widetilde{M}^{22l_4/(3l_5)}\right]^{l_5}}\quad \mathrm{erg\,s^{-1}}, \tag{35}$$

where

$$l_1 = 2.777,\ l_2 = 25.13,\ l_3 = 3.095,\ l_4 = 7.585,\ l_5 = 7.381. \tag{36}$$

The maximum error of the fitting expressions (33) and (35) does not exceed 14 per cent. Unfortunately, these two approximations do not match at $M = 1.3\,\mathrm{M}_\odot$. Thus, to calculate the neutrino emissivity for a white dwarf with the mass $M \in [1.28, 1.32\,\mathrm{M}_\odot]$, we recommend to use a linear interpolation

$$L_{\nu3}(M,T) = L_{\nu1}(1.28\,\mathrm{M}_\odot, T) + \frac{L_{\nu2}(1.32\,\mathrm{M}_\odot,T) - L_{\nu1}(1.28\,\mathrm{M}_\odot,T)}{0.04}(\widetilde{M}-1.28). \tag{37}$$

This interpolation does not affect the maximum fitting error which remains to be 14 per cent at $T = 2.38\times10^8$ K and $M = 1.34\,\mathrm{M}_\odot$.

As seen from equations (33) and (35), in the limit of high temperatures $L_\nu \sim T^3$, while in the limit of low temperatures $L_\nu \sim T^{31/3}$. Let us demonstrate how to obtain this temperature dependence from simple physical arguments.

At high temperatures, the internal stellar temperature T is much greater than the plasma frequency $\omega_{\mathrm{p}0}$ in the centre of the star. Since the plasma frequency of degenerate electrons becomes smaller as the density decreases (see equation 7), we have $k_\mathrm{B}T \gg \hbar\omega_\mathrm{p}$ throughout the star. In this case the neutrino emissivity of an arbitrary volume element in the star is given by asymptote (28) and the luminosity equals

$$L_\nu \approx 4\xi_3\,\frac{\hbar^6 k_\mathrm{B}^3}{(m_\mathrm{e}c^2)^9}\,Q_0 T^3\int_\mathrm{star}\beta^6\,\omega_\mathrm{p}^6\,\mathrm{d}V. \tag{38}$$

Here the integral is taken over the volume V of the star. Since the plasma frequency ω_p and the parameter β depend only on $\tilde{\rho}$ (see equations 7 and 12), one gets $L_\nu \propto T^3$.

In the low-temperature limit, when $k_\mathrm{B}T \ll \hbar\omega_{\mathrm{p}0}$, the main contribution to the luminosity comes from a thin spherical layer of width h, in which $\hbar\omega_\mathrm{p} \sim k_\mathrm{B}T$. This layer is situated in the outermost part of the stellar core, where the electrons form a degenerate, non-relativistic gas. Indeed, if we move from this layer to the stellar centre, ω_p will increase while the emissivity will be exponentially suppressed, $Q \sim \exp(-\hbar\omega_\mathrm{p}/k_\mathrm{B}T)$, in accordance with equation (29). If we move from the layer to the stellar surface then the emissivity will also decrease (see asymptote 28) but in a power-law fashion, $Q \sim \beta^6\omega_\mathrm{p}^6 = \omega_\mathrm{p}^6(\beta = 1$ for the non-relativistic electron gas, see equation 12). Therefore, the emissivity will have a maximum in a layer in which $\hbar\,\omega_\mathrm{p} \sim k_\mathrm{B}\,T$, and the neutrino luminosity of a star can be estimated as

$$L_\nu \sim 4\xi_3\beta^6\,Q_0\left(\frac{k_\mathrm{B}T}{m_\mathrm{e}c^2}\right)^9\left(\frac{\hbar\omega_\mathrm{p}}{k_\mathrm{B}T}\right)^6 4\pi R^2 h$$
$$\sim 16\pi\xi_3\,Q_0\left(\frac{k_\mathrm{B}T}{m_\mathrm{e}c^2}\right)^9 R^2 h, \tag{39}$$

where R is the white dwarf radius. An order of magnitude estimate gives the characteristic width h of the layer, $h \sim \omega_\mathrm{p}^6/(\mathrm{d}\,\omega_\mathrm{p}^6/\mathrm{d}\,r)$. Using the hydrostatic equilibrium equation and the scaling relations for the plasma frequency (see equation 7) $\omega_\mathrm{p} \propto \tilde{\rho}^{1/2}$ and pressure $P \propto \tilde{\rho}^{5/3}$ of the degenerate non-relativistic gas, we get $h \propto \tilde{\rho}^{2/3} \propto \omega_\mathrm{p}^{4/3} \propto T^{4/3}$. Consequently, $L_\nu \propto T^{31/3}$ in agreement with the estimate (39).

Let us note that the plasmon decay neutrino emissivity and hence the luminosity of the star depends on the effective density $\tilde{\rho}$, which is related to the real density ρ by equation (3), $\tilde{\rho}/\rho = 1/\mu_\mathrm{e} = \sum_i Z_i n_i/(\sum_i A_i n_i)$. In white dwarfs with any reasonable chemical composition, the mass number A_i of atomic nuclei species i is always twice as much than the charge number Z_i (recall that we neglect beta-captures). Thus, the ratio $\tilde{\rho}/\rho$ is equal to 1/2. We used this ratio in all our calculations.

6 SUMMARY

We have calculated the neutrino emissivity Q due to plasmon decay in an electron–positron plasma making no assumptions about degree of degeneracy or relativity of the electron gas.

When calculating the emissivity one needs the plasma dielectric functions as well as the dispersion relations for transverse and longitudinal plasmons in a wide range of temperatures and densities. In particular, we have calculated the plasma frequency ω_p and fitted it by an analytical formula. This formula reproduces the main asymptotes for ω_p (degenerate, ultrarelativistic or non-degenerate non-relativistic electrons, see Section 3).

The results of numerical calculations of the neutrino emissivity were also approximated by a convenient analytical expression. It satisfies the asymptotes in various limiting cases (Section 4, also see the paper by Braaten & Segel 1993). The approximation is valid for $T = 10^7$–10^{11} K and $\tilde{\rho} = (2 \times 10^2$–$10^{14})$ g cm^{-3}. The rms relative error of the approximation does not exceed 4 per cent for those temperatures and densities, for which $f = \hbar\omega_{\rm p}/(k_{\rm B}T) < 20$ [while at $f > 20$ the emissivity is exponentially small, $Q \sim \exp(-f)$].

The fitting expression for the emissivity was used to calculate the neutrino luminosity of white dwarfs (Section 5). This neutrino luminosity was fitted by analytic formulae and presented as a function of white dwarf mass and its internal temperature. It is shown that the neutrino luminosity depends on the chemical composition of a white dwarf only through the parameter $\mu_{\rm e}$ which is equal to 2 for reasonable white dwarf compositions.

The results of this paper can be used in a number of applications, in particular, in modelling of the evolution of red giants or pre-supernovae as well as in the cooling theory of white dwarfs (see e.g. Haft et al. 1994; Winget et al. 2004).

ACKNOWLEDGMENTS

The authors are grateful to D. G. Yakovlev for discussions; to our referee, Agnes Kim, for valuable suggestions and comments; to A. I. Chugunov for providing the code that was used to approximate numerical results by analytical functions; to A. Y. Potekhin for calculating the relation between the surface and internal temperatures of helium atmosphere white dwarfs; and to D. P. Barsukov and A. M. Krassilchtchikov for technical assistance. This research was supported by RFBR (grants 05-02-16245 and 05-02-22003) and by the Federal Agency for Science and Innovations (grant NSh 9879.2006.2).

REFERENCES

Adams J. B., Ruderman M. A., Woo C.-H., 1963, Phys. Rev., 129, 1383
Braaten E., 1991, Phys. Rev. Lett., 66, 1655
Braaten E., Segel D., 1993, Phys. Rev. D, 48, 1478
Haft M., Raffelt G., Weiss A., 1994, ApJ, 425, 222
Itoh N., Mutoh H., Hikita A., Kohyama Y., 1992, ApJ, 395, 622
Jancovici B., 1962, Nuovo Cimento, 25, 428
Kohyama Y., Itoh N., Obama A., Hayashi H., 1994, ApJ, 431, 761
Landau L. D., Lifshitz E. M., 1980, Course of Theoretical Physics, Part I, Statistical Mechanics. Pergamon Press, Oxford
Odrzywołek A., 2007, Eur. Phys. J. C, in press (doi:10.1140/epjc/s10052-007-0378-4) (arXiV:0704.1222)
Winget D. E., Sullivan D. J., Metcalfe T. S., Kawaler S. D., Montgomery M. H., 2004, ApJ, 602, L109
Yakovlev D. G., Kaminker A. D., Gnedin O. Y., Haensel P., 2001, Phys. Rep., 354, 1

APPENDIX A: DIELECTRIC FUNCTIONS OF ELECTRON–POSITRON PLASMA

Using the density matrix formalism we calculated the dielectric function of the electron–positron gas in the first order of perturbation theory. The longitudinal $\varepsilon_{\rm l}(\omega, k)$ and transverse $\varepsilon_{\rm t}(\omega, k)$ components of the dielectric tensor can be written in the form ($c = \hbar = k_{\rm B} = 1$)

$$\varepsilon_{\rm l} = 1 - \frac{4\pi\alpha}{\omega^2} \sum_{\rm e^-, e^+} \int \frac{{\rm d}^3\boldsymbol{p}}{(2\pi)^3} \frac{1}{E_{\boldsymbol{p}+\boldsymbol{k}} E_{\boldsymbol{p}}} \frac{n_{\boldsymbol{p}+\boldsymbol{k}} - n_{\boldsymbol{p}}}{E_{\boldsymbol{p}+\boldsymbol{k}} - E_{\boldsymbol{p}} - \omega - {\rm i}\delta} \times \left[2\frac{(\boldsymbol{p}\cdot\boldsymbol{k})^2}{k^2} + (\boldsymbol{p}\cdot\boldsymbol{k}) + E_{\boldsymbol{p}+\boldsymbol{k}} E_{\boldsymbol{p}} - E_{\boldsymbol{p}}^2 \right], \quad (A1)$$

$$\varepsilon_{\rm t} = 1 - \frac{4\pi\alpha}{\omega^2} \sum_{\rm e^-, e^+} \int \frac{{\rm d}^3\boldsymbol{p}}{(2\pi)^3} \frac{1}{E_{\boldsymbol{p}+\boldsymbol{k}} E_{\boldsymbol{p}}} \frac{n_{\boldsymbol{p}+\boldsymbol{k}} - n_{\boldsymbol{p}}}{E_{\boldsymbol{p}+\boldsymbol{k}} - E_{\boldsymbol{p}} - \omega - {\rm i}\delta} \times \left[\frac{(\boldsymbol{p}\times\boldsymbol{k})^2}{k^2} - (\boldsymbol{p}\cdot\boldsymbol{k}) + E_{\boldsymbol{p}+\boldsymbol{k}} E_{\boldsymbol{p}} - E_{\boldsymbol{p}}^2 \right]. \quad (A2)$$

Here, the summation is carried over electrons and positrons; $n_{\mathbf{p}} = 1/[\exp(E_{\boldsymbol{p}} \mp \mu)/T + 1]$ is the Fermi–Dirac distribution function for electrons (in this case one has to choose the sign $-$) or positrons (the sign $+$); $E_{\boldsymbol{p}} = \sqrt{\boldsymbol{p}^2 + m_{\rm e}^2}$ and $E_{\boldsymbol{p}+\boldsymbol{k}} = \sqrt{(\boldsymbol{p}+\boldsymbol{k})^2 + m_{\rm e}^2}$ are the energies of an electron or a positron with momenta $\boldsymbol{p}$ and $\boldsymbol{p} + \boldsymbol{k}$, respectively.

We have checked that equations (A1) and (A2) are equivalent to corresponding expressions for the dielectric function which can be obtained from the polarization tensor $\Pi^{\mu\nu}$ of Braaten & Segel (1993) (see their equation A1).

The integration over the angles in equations (A1) and (A2) can be done analytically. As a result, one obtains for real parts of $\varepsilon_{\rm l}$ and $\varepsilon_{\rm t}$,

$$\varepsilon_{\rm l} = 1 - \frac{\alpha}{\pi\omega^2} \int_0^\infty {\rm d}p\ p^2 \left[n_{\rm F}(E_{\rm p}) + \overline{n}_{\rm F}(E_{\rm p}) \right] R_{\rm l}, \quad (A3)$$

$$\varepsilon_{\rm t} = 1 - \frac{\alpha}{\pi\omega^2} \int_0^\infty {\rm d}p\ p^2 \left[n_{\rm F}(E_{\rm p}) + \overline{n}_{\rm F}(E_{\rm p}) \right] R_{\rm t}, \quad (A4)$$

where

$$R_{\mathrm{l}} = -\frac{4\omega^2}{E_{\mathrm{p}}k^2} + \frac{\omega^2}{2E_{\mathrm{p}}k^3 p}\left[(2E_{\mathrm{p}}+\omega)^2 - k^2\right]\ln\left|\frac{E_{p-k}^2-(E_{\mathrm{p}}+\omega)^2}{E_{p+k}^2-(E_{\mathrm{p}}+\omega)^2}\right| + \frac{\omega^2}{2E_{\mathrm{p}}k^3 p}\left[(2E_{\mathrm{p}}-\omega)^2 - k^2\right]\ln\left|\frac{E_{p-k}^2-(E_{\mathrm{p}}-\omega)^2}{E_{p+k}^2-(E_{\mathrm{p}}-\omega)^2}\right|, \tag{A5}$$

$$R_{\mathrm{t}} = \frac{2(\omega^2+k^2)}{E_{\mathrm{p}}k^2} + \frac{1}{4E_{\mathrm{p}}k^3 p}\left[k^4+4k^2p^2+4k^2E_{\mathrm{p}}\omega - \omega^2(2E_{\mathrm{p}}+\omega)^2\right]\ln\left|\frac{E_{p-k}^2-(E_{\mathrm{p}}+\omega)^2}{E_{p+k}^2-(E_{\mathrm{p}}+\omega)^2}\right| + \frac{1}{4E_{\mathrm{p}}k^3 p}\left[k^4+4k^2p^2-4k^2E_{\mathrm{p}}\omega - \omega^2(2E_{\mathrm{p}}-\omega)^2\right]\ln\left|\frac{E_{p-k}^2-(E_{\mathrm{p}}-\omega)^2}{E_{p+k}^2-(E_{\mathrm{p}}-\omega)^2}\right|. \tag{A6}$$

In equations (A3)–(A6) $n_{\mathrm{F}}(E_{\mathrm{p}})$ and $\overline{n}_{\mathrm{F}}(E_{\mathrm{p}})$ are the Fermi–Dirac distribution functions for electrons and positrons, respectively; $E_{p\pm k} = \sqrt{(p\pm k)^2+m_{\mathrm{e}}^2}$ is the energy of an electron or a positron with the absolute value of momentum equal to $(p \pm k)$.

Knowing the dielectric functions, the plasmon dispersion relations can be found from the equations

$$\varepsilon_{\mathrm{l}}(\omega,k) = 0, \qquad \omega^2\,\varepsilon_{\mathrm{t}}(\omega,k) = k^2. \tag{A7}$$

If the electron gas is completely degenerate ($T = 0$), then the integrals in equations (A3) and (A4) can be taken analytically. The result is

$$\varepsilon_{\mathrm{l}} = 1 - \frac{\alpha}{\pi}\left\{ -\frac{8}{3}\frac{1}{k^2}\,p_{\mathrm{F}}\sqrt{p_{\mathrm{F}}^2+m_{\mathrm{e}}^2} + \frac{2}{3}\sinh^{-1}\frac{p_{\mathrm{F}}}{m_{\mathrm{e}}} + \frac{1}{3}\frac{(k^2-\omega^2-2m_{\mathrm{e}}^2)}{(k^2-\omega^2)}\sqrt{\frac{k^2-\omega^2+4m_{\mathrm{e}}^2}{\omega^2-k^2}}\;L_1 - \frac{1}{6k^3}\sqrt{p_{\mathrm{F}}^2+m_{\mathrm{e}}^2}\left(3\omega^2-3k^2+4p_{\mathrm{F}}^2+4m_{\mathrm{e}}^2\right)L_2 + \frac{\omega}{12k^3}\left(\omega^2-3k^2+12p_{\mathrm{F}}^2+12m_{\mathrm{e}}^2\right)L_3 \right\}, \tag{A8}$$

$$\varepsilon_{\mathrm{t}} = 1 - \frac{\alpha}{\pi\omega^2}\left\{ \frac{2}{3}\frac{(k^2+2\omega^2)}{k^2}\,p_{\mathrm{F}}\sqrt{p_{\mathrm{F}}^2+m_{\mathrm{e}}^2} - \frac{2}{3}(k^2-\omega^2)\sinh^{-1}\frac{p_{\mathrm{F}}}{m_{\mathrm{e}}} - \frac{(k^2-\omega^2-2m_{\mathrm{e}}^2)}{3}\sqrt{\frac{k^2-\omega^2+4m_{\mathrm{e}}^2}{\omega^2-k^2}}\;L_1 + \frac{\sqrt{p_{\mathrm{F}}^2+m_{\mathrm{e}}^2}}{k^3}\left[-\frac{1}{3}(k^2-\omega^2)(p_{\mathrm{F}}^2+m_{\mathrm{e}}^2) + \frac{1}{4}\left(-k^4+\omega^4+4m_{\mathrm{e}}^2k^2\right)\right]L_2 + \frac{\omega}{24k^3}\left[(k^2-\omega^2)\left(3k^2+\omega^2+12p_{\mathrm{F}}^2+12m_{\mathrm{e}}^2\right) - 12m_{\mathrm{e}}^2k^2\right]L_3 \right\}. \tag{A9}$$

The quantities L_2 and L_3 are

$$L_2 = \ln\left|\frac{(-k^2+\omega^2-2kp_{\mathrm{F}})^2 - 4\omega^2(p_{\mathrm{F}}^2+m_{\mathrm{e}}^2)}{(-k^2+\omega^2+2kp_{\mathrm{F}})^2 - 4\omega^2(p_{\mathrm{F}}^2+m_{\mathrm{e}}^2)}\right|, \tag{A10}$$

$$L_3 = \ln\left|\frac{(-k^2+\omega^2)^2 - 4(\omega\sqrt{p_{\mathrm{F}}^2+m_{\mathrm{e}}^2}+kp_{\mathrm{F}})^2}{(-k^2+\omega^2)^2 - 4(\omega\sqrt{p_{\mathrm{F}}^2+m_{\mathrm{e}}^2}-kp_{\mathrm{F}})^2}\right|. \tag{A11}$$

The quantity L_1 depends on the sign of $D \equiv (\omega^2 - k^2)(k^2 - \omega^2 + 4\,m_e^2)$. At $D \geqslant 0$ one has

$$
\begin{aligned}
L_1 = \arctan &\left[\frac{-2m_e k p_F + \left(k^2 + 2m_e\omega - \omega^2\right)\left(\sqrt{p_F^2 + m_e^2} - m_e\right)}{p_F \sqrt{(\omega^2 - k^2)\left(k^2 - \omega^2 + 4m_e^2\right)}} \right] \\
+ \arctan &\left[\frac{2m_e k p_F + \left(k^2 + 2m_e\omega - \omega^2\right)\left(\sqrt{p_F^2 + m_e^2} - m_e\right)}{p_F \sqrt{(\omega^2 - k^2)\left(k^2 - \omega^2 + 4m_e^2\right)}} \right] \\
+ \arctan &\left[\frac{-2m_e k p_F + \left(k^2 - 2m_e\omega - \omega^2\right)\left(\sqrt{p_F^2 + m_e^2} - m_e\right)}{p_F \sqrt{(\omega^2 - k^2)\left(k^2 - \omega^2 + 4m_e^2\right)}} \right] \\
+ \arctan &\left[\frac{2m_e k p_F + \left(k^2 - 2m_e\omega - \omega^2\right)\left(\sqrt{p_F^2 + m_e^2} - m_e\right)}{p_F \sqrt{(\omega^2 - k^2)\left(k^2 - \omega^2 + 4m_e^2\right)}} \right].
\end{aligned}
\tag{A12}
$$

At $D < 0$

$$
L_1 = \frac{\mathrm{i}}{2} \ln \left| \frac{\left[(k^2 - \omega^2)\sqrt{p_F^2 + m_e^2} + p_F \sqrt{(k^2 - \omega^2)(k^2 - \omega^2 + 4m_e^2)}\right]^2 - 4m_e^4\omega^2}{\left[(k^2 - \omega^2)\sqrt{p_F^2 + m_e^2} - p_F \sqrt{(k^2 - \omega^2)(k^2 - \omega^2 + 4m_e^2)}\right]^2 - 4m_e^4\omega^2} \right|. \tag{A13}
$$

Note that equations (A8) and (A9) for the dielectric functions agree with the well-known results of Jancovici (1962) only at $D < 0$ (see his equations A1 and A4). At $D \geqslant 0$ his expressions (A1) and (A4) are formally inapplicable (the real part of the dielectric functions in these equations becomes complex). In this case one should use our equations (A8) and (A9).

In addition, it may be useful to note that the Jancovici's definition of the transverse dielectric function differs from a generally accepted one. His dielectric function $\varepsilon_t^{\mathrm{Janc}}$ is related to our dielectric function by $\varepsilon_t^{\mathrm{Janc}} = (k^2 - \omega^2\,\varepsilon_t)/(k^2 - \omega^2)$.

APPENDIX B: DESCRIPTION OF A TABLE OF OUR NUMERICAL RESULTS

The results of our numerical calculations are summarized in the table (file table.dat) which can be found on the web site http://www.ioffe.ru/astro/NSG/plasmon/table.dat.

The table consists of seven columns. In the first column, we present log T (in K); in the second column we give $\log(\tilde{\rho}) = \log(\rho/\mu_e)$ (g cm^{-3}); in the third and fourth columns we present, respectively, the emissivities Q_t and Q_l (erg s^{-1} cm^{-3}) due to decay of transverse and longitudinal plasmons; the fifth column is the plasma frequency ω_p (s^{-1}), which is numerically calculated from the exact dispersion relations (A7) (not using the Braaten–Segel approximation); the sixth column is the same plasma frequency but calculated from equation (5) (the Braaten–Segel approximation). Finally, in the seventh column we present the characteristic dimensionless velocity of electrons $v_* = \omega_1/\omega_p$ in units of c, calculated in the Braaten–Segel approximation (i.e. by making use of equations 5 and 9 for ω_p and ω_1, respectively).

This paper has been typeset from a TEX/LATEX file prepared by the author.